International Journal of Modern Engineering Research (IJMER)
www.ijmer.com Vol. 2, Issue. 5, Sept.-Oct. 2012 pp-2998-3005 ISSN: 2249 6645

Group features of small seismic waveforms

Wenlong Liu[1], Yucheng Liu[2]
Shanghai Earthquake Administration, Shanghai, China, 200062
Department of Mechanical Engineering
University of Louisiana, Lafayette, LA70504, USA

Abstract: *This paper demonstrates several group features observed from small seismic waveforms and distinguishes abnormal group features that preceded destructive major shocks from normal ones. Important group features discussed in this paper include direction of seismic wave's first motion, amplitude ratio, half period of the first motion, frequency components of earthquakes, and linearity of seismic waveform. The group features illustrated in this paper have been used as important criteria in earthquake prediction.*

Keywords: *first motion, amplitude ratio, linearity of seismic waveform, consistency, earthquake prediction*

I. Introduction

It was learned from numerous earthquake examples that abnormal group features of seismic waves of small earthquakes are usually signs of strong major earthquakes. Therefore, in earthquake prediction, the features and information carried by small seismic waves need to be thoroughly investigated to determine seismic tendency in certain area. This paper presents reveals the correlations between the major shock and several seismic wave features, including direction of the first motion, amplitude ratio, half period of the first motion, frequency components of foreshocks, and linearity of seismic waveform. The illustrative examples and methods introduced in this paper can be used as significant tools in future earthquake prediction.

II. Consistency of Directions of the First Motion

To determine if strong earthquakes will occur in the future based on the consistency of first motion of P waves of small and micro earthquake sequences that are recorded by the seismic observatories that are near to the epicenter was firstly found and applied by the author when he was analyzing the Huoshan earthquake cluster in Anhui Province. An earthquake cluster occurred in Huoshan County in March of 1973, the largest earthquake was M_L4.5 that occurred on March 11th. Two large earthquakes occurred before that one, one of them was a M_L4.3 earthquake that just occurred eight minutes before the largest shock and the other one was M_L3.1 that occurred on March 7th. After the largest shock, another comparatively strong earthquake occurred on March 12th, whose magnitude was M_L4.0. Since then, this earthquake cluster attenuated with ups and downs. At that time, the author worked at Fuziling seismic observatory, which was only about 10km from the epicenter. In analyzing seismograms, it was found that before the M_L4.5 earthquake, the vertical direction of the initial motion of P waves was downward most of time, except for the short time span after the M_L3.1 earthquake, during which the direction was upward (the initial motion direction at the time that M_L3.1 occurred was also downward). However, that direction was upward on March 12th when M_L4.0 occurred and since then the direction was in disorder. Meanwhile, several other observations were made by the author. (1) Ts-p of small and micro earthquakes before the M_L4.5 earthquake was consistent, which was 1.3 seconds. After the M_L4.0 earthquake, Ts-p varied from 1.1 ~ 1.5 seconds, which indicated a diffusion of the epicentral distribution range. (2) Before the M_L4.5 earthquake, especially before March 7th, the daily frequency of the small and micro earthquakes unconventionally increased day by day and a notable swarm-equanimity phenomenon accompanied. Such daily frequency ceased increasing after the M_L4.0 earthquake. (3) Before the M_L4.5 earthquake, especially before March 7th, the magnitude of small earthquakes gradually rose. Based on above observations, the author determined that the M_L4.5 earthquake must be the largest shock and there would not be any stronger shock occurs after that, which had been proven right. These phenomena recurred in later earthquakes, and the most famous example is the M7.3 Haicheng earthquake. Haicheng earthquake is a massive earthquake with direct foreshock sequence. As recorded by Shipengyu station (Ts-p was 2.5 seconds), in its foreshock sequence, 79 shocks had identifiable initial motion direction and 78 of them had a downward direction. However, such direction was disorderly after the main shock [1]. Haicheng earthquake was the first and the only successful earthquake prediction in history and based on the prediction, Chinese government was able to successfully evacuate much of the populace and furthest mitigate the disaster caused by that earthquake. An essential key of this successful prediction was correctly identifying its foreshock sequence and the consistency of P wave's initial motion direction provided a primary basis for that. Since then, this method became one of most popular methods in judging if a sequence is a foreshock sequence and whether or not strong earthquakes will occur after that.

Table 1. Distribution of initial motion of P waves of Huoshan earthquake swarm (occurred in March of 1973) recorded by Fuziling station (N is the number of earthquakes whose initial motion direction was identifiable, N_U is the number of earthquakes with upward initial motion, N_L is the number of earthquakes with downward motion and % is its percentage, B means before the main shock, and A means after the main shock)

Date (03/x)	4~6	7			8	9	10	11			12			13	14	15	16	17~31
		B	M_L 3.1	A				M_L4.3	M_L4.5	A	B	M_L4.0	A					
N	19	28		23	5	13	4			55	30		13	14	11	7	5	31
N_U	0	2		8	1	0	0			14	13		6	6	3	4	2	15
N_L	19	26	X	15	4	13	4	X	X	41	17	X	7	8	8	3	3	16
%	100	92.9		65.2	80	100	100			74.5	56.7		53.8	57.1	72.7	42.9	60	51.6

Using consistency of P wave's initial motion direction to predict future earthquakes is simple and convenient but in some cases, false prediction could be made if only using that method. For example, in July of 1979, small earthquake activities took place in Huoshan with the maximum magnitude M2.2 (occurred at 21:00 on July 8th). During that earthquake swarm, overall 27 earthquakes with identifiable initial motion direction were recorded by Fuziling seismic station and it was found that all the earthquakes had a downward initial motion direction except for the one occurred on July 9th. Moreover, the initial motion directions of all 84 small earthquakes recorded by Huoshan seismic station were downward. Therefore, we cannot determine the occurrence of stronger earthquakes only based on the consistency of the initial motion direction and other seismic indicators need to be synthetically analyzed in order to attain accurate predictions. Meanwhile, not every local station can accurately reflect variation of the initial motion direction of small earthquakes. For example, in the Wencheng earthquake swarms (1.2.2), after the maximum earthquake (M_L4.6), a consistency of P wave's initial motion direction of the small earthquakes was found according to the records in nearby stations (Hangzhou, Wenzhou, etc.), which became a strong proof that foreboded occurrence of stronger earthquakes. However, it was proven that these stations failed to detect the initial motion direction because they are not close enough to the fault lines. Actually, turbulence of the initial motion direction was only detected by the Xinpuxiang station, a new seismic station established after the earthquake swarms started (7km from the epicenter), after the M_L4.6 earthquake. Finally, for those dual-shock-type earthquakes (the magnitude difference between the first main shock (the strongest earthquake) and the second main shock (the second strongest earthquake) is less than 0.3), two groups of small shocks with different fault plane solutions usually occur between the two main shocks. The initial motion direction of the two groups of small shocks may not be consistent. In that case, even the initial motion direction is in disorder, another strong earthquake (the second main shock in a dual-shock-type earthquake) will still occur after the first main shock. Such mechanism is the same as that of the consistency of focal mechanism solutions before mid-strong earthquakes.

III. Consistency of Amplitude Ratio

Amplitude ratio of an earthquake is the ratio between its P wave's maximum vertical amplitude and its S wave's maximum vertical amplitude. Those amplitudes must be recorded by the same instrument. A number of earthquake examples showed that the amplitude ratio of those small earthquakes which occurred before the largest earthquake in a foreshock sequence or an earthquake swarm was fairly consistent. However, that value highly dispersed after the largest earthquake. Fig. 1presents an example, which is taken from the Haicheng earthquake [2]. Thus, the consistency of amplitude ratio became a popular and effective criterion in deciding whether or not a larger earthquake will occur in the future.

Compare to the mechanism of consistency of amplitude ratio of the small earthquakes, the mechanism of those mid-strong earthquakes is more complicated because it also depends on the medium characteristics. Feng [3] used two-layer crust model and synthetically studied the influences of focal force systems and media on the amplitude ratio. According to Feng, several conclusions were drawn. (1) Amplitude ratio is proportional to the square of the wave velocity ration. Therefore it is possible to observe a visible decrease in the seismic waves that transmitted through the seismogenic zones within quite a long period of time before the main shock. (2) Generally, direction of hypocentral force system considerably affects the amplitude ration. However, such influence is not noticeable for a vertical fault plane that has tangential dislocation. Thus, in earthquake prediction practice, we often compare the amplitude ratios of neighboring earthquakes to attain an accurate prediction. (3) Variation of the amplitude ratio in near-source regions along with hypocentral distance is very intricacy and the amplitude ratio is seriously affected by the azimuth angle. Thus, it is better to use the data recorded by some distant seismic stations, whose distance from the hypocenter ranges from 70 to 100km.

IV. Half Period of Initial Motion

In April 6th of 1976, a M_L6.3 earthquake occurred in Hellinger, Inner Mongolia. From the records of Shenliying station (hypocentral distance is about 30km), it was found that among the small and micro earthquakes with consistent initial motion which occurred from April 4th to 8th, 70% of them had a half period of initial motion about 0.1 seconds and only a few of them had 0.2-second half period. However, after April 8th, the number of earthquakes whose half period was 0.1 seconds gradually decreased and the number of earthquakes with 0.2-second half period increased fast [4]. Such trend was also

observed from the data recorded by other local stations. The author also found this phenomenon in his works. For example, in the M_L5.0 Guzhen earthquake which occurred in March 2nd of 1979, the half period of initial motion of its foreshocks was clearly shorter than that of its aftershocks (according to records of Jiashan station). Guzhen earthquake only had a few fore- and aftershocks. The magnitude of the largest foreshock was M_L3.2 and the magnitude of the largest aftershock was M_L3.5. This feature was used by the author in quickly and correctly forecasting the Wencheng earthquake sequence [5, 6].

If the magnitudes are comparable, the half period of initial motion of the foreshock is less than that of the aftershock. Those periods have to be recorded by same station (neglecting the instrumental interference). Such mechanism can have several explanations. Assume the energy released by earthquake is

$$E = \Delta\sigma \cdot D \cdot S \qquad (1)$$

where$\Delta\sigma$ is stress drop, D is average dislocation on rupture surfaces, and S is area of the rupture surface. Since the energies released by the earthquakes with comparable magnitudes are close to each other, the less half period of initial motion of the foreshock indicates a smaller area (S) of rupture surface of the fore shock. This means that the energy per unit surface area released during the foreshocks is larger than that released during the aftershocks. In another word, $\Delta\sigma \cdot D$ of the foreshocks is higher than that of the aftershocks. Assuming that D and friction of rupture surface of the foreshocks and aftershocks are roughly the same, it can be deduced that the foreshocks lead to higher ambient stress. Also, for those strong main shocks with high magnitudes, fragmentation of media close to the epicenters may be caused after the main shocks, the Q value will be lowered and more high frequency waves well be absorbed, the half period of initial motion of the aftershock is therefore increased. In addition, for the foreshocks occur under a high effective stress, the rupture will be transmitted at a high speed, which intensifies high frequency radiation and effects of directivity [7, 8]. Like other prediction methods, counter examples were also observed. For instance, it was report that the M_L5.7 Oroville earthquake occurred in August 1st, 1985, the half period of initial motion of its foreshock was longer that of its aftershock [9]. This example revealed that during earthquakes, the mechanisms of its focal force system and distribution of medium are very intricate.

V. Frequency Components

It has been well accepted that foreshocks have abundant high-frequency components. As observed by Sadovsky et al. [10, 11], in the large processes preceding large earthquakes (M = 4.5 ~ 5.8) in the region of Garm, a change in the frequency spectrum of microshocks took place and the percentage of high-frequency shocks increased. Ishida and Kanamori [12] found that the frequency of the spectral peak was systematically higher for the foreshocks than the events prior to 1949 in the small earthquakes preceding the 1952 Kern County, California, earthquake. A similar trend was also found for the 1971 San Fernando earthquake and micro shocks in the region of Xikeer, Xinjiang [13, 14]. Fig. 1 and Table 2 display four small earthquake sequences in the region of Xikeer, Xinjiang. As shown in Table 3, earthquakes in sequence 1, 2, and 3 that occurred before and after the maximum earthquake were grouped in chronological order; earthquakes in sequence 4 were separated into two groups because there was no maximum earthquake in that sequence. Fig. 2 plots average frequency spectra of the four small earthquake sequences occurred in the region of Xikeer. As shown from that figure, the spectrum component between 10Hz and 60Hz increased by 15% during six months before the largest earthquakes in the first three small earthquake sequences. Such variation was not obvious in the fourth sequence. Dominant frequencies of the first three earthquake sequences were about 10Hz and that of the fourth sequence was lower than 6Hz.

For earthquakes with comparable magnitudes, spectra of the foreshocks include more high-frequency component than those of the aftershocks. This mechanism is basically the same as that that governs the half period of initial motion of the foreshocks and aftershocks discussed before. The shorter half period of initial motion of the foreshocks is the reflection of that mechanism in the time domain and the more high-frequency component in the foreshocks is its reflection in the frequency domain.

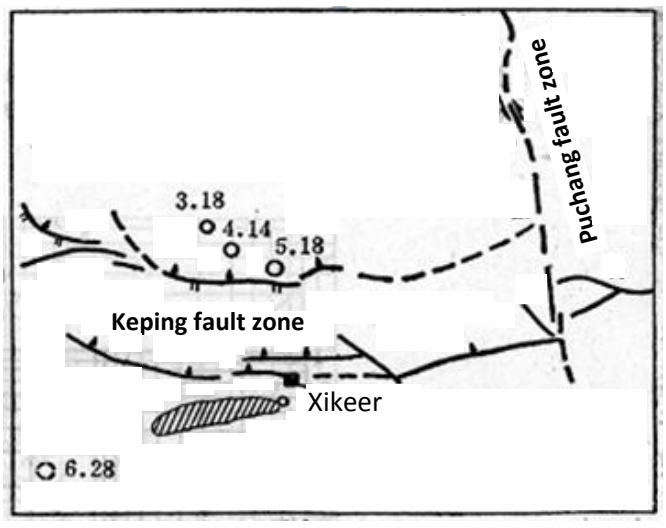

Figure 1. Locations of four small earthquake sequences and local seismic stations in the region of Xikeer

Table 2. Four small earthquake sequences in Xikeer

No.	Duration (in 1972)	Ts-p	M_L	Number of maximum earthquakes						No. of earthquakes
				Time	Ts-p	M_L	Φ_N	λ_E	h (km)	
1	2.11~3.26	2.0~3.0	1.0~2.0	22:37:35.9 on 3.18	2.7	3.7	39°58’	77°15’	25	53
2	3.19~5.23	2.5~3.6	1.0~2.0	19:15:53.9 on 4.14	3.5	4.2	39°57’	77°17’	25	48
3	3.1~5.23	1.5~2.0	0.6~1.0	08:43:42.6 on 5.18	1.7	3.2	39°56’	77°21’	25	45
4	3.29~12.1	4.0~4.6	0.6~1.7	11:05:00 on 6.28	4.5	1.7	Azimuth angle 246°		25	26

Table 3. Grouping of earthquake sequences in Xikeer (the second column lists earthquake groups, third column displays duration of each group, and the fourth column shows number of earthquakes in each group)

1				2				3			4	
A_{13}	A_{12}	A_{11}	B_{11}	A_{22}	A_{21}	B_{21}	B_{22}	A_{32}	A_{31}	B_{31}	C_{41}	C_{42}
2.11~2.13	2.14~2.29	3.5~3.17	3.19~3.26	3.19~3.31	4.1~4.14	4.14~4.20	4.21~5.23	3.1~4.7	5.2~5.18	5.18~5.23	3.29~4.30	6.28~12.1
11	11	11	9	9	10	11	17	19	15	10	13	13

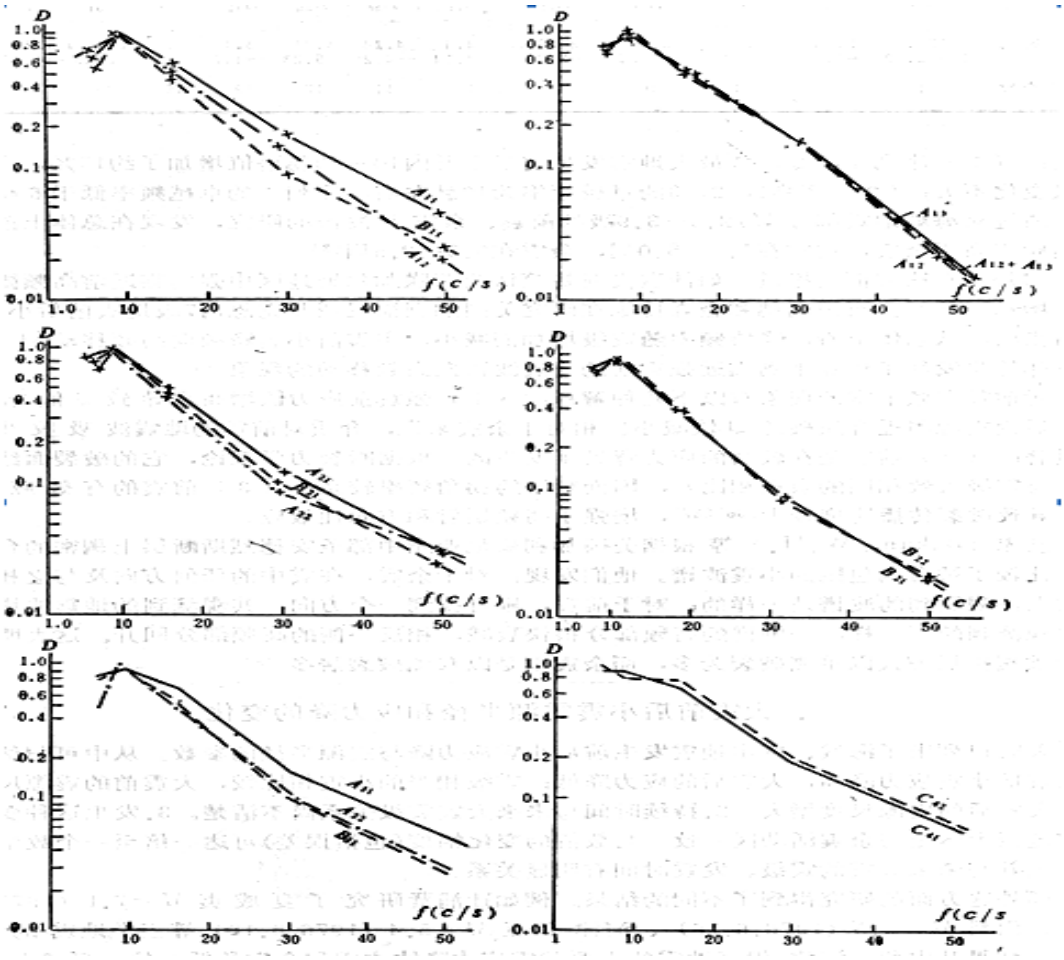

Figure 2. Average frequency spectra of four small earthquake sequences in Xikeer

VI. Linearity of Seismic Waveform

Feng et al. [15] presented temporal and spatial linearity of seismic waveforms from the perspective of system science. Based on Feng's definition, a certain number of time t_1, t_2, …,t_n at which the amplitude of displacement or velocity reaches its peak, trough, or zero point are recorded since the P-wave or S-wave initial-motion until one or two wave groups end or n reaches a certain value N. After that, the t_i-irelationship can be drawn in a coordinate system whose ordinate is t_i and abscissa is the index number i, and the linear correlation coefficient r can be calculated using least square method as:

$$r = \frac{S_{ti}}{\sqrt{S_{tt} \cdot S_{ii}}} \tag{2}$$

where

$$\left.\begin{aligned} S_{ti} &= \sum_{i=1}^{n} \left(t_i - \bar{t}\right)\left(i - \frac{n+1}{2}\right) \\ S_{tt} &= \sum_{i=1}^{n} \left(t_i - \bar{t}\right)^2 \\ S_{ii} &= \sum_{i=1}^{n} \left(i - \frac{n+1}{2}\right)^2 \\ \bar{t} &= \frac{1}{n}\sum_{i=1}^{n} t_i \end{aligned}\right\} \tag{3}$$

Here r is the temporal linearity of seismic waveforms, and the more the waveforms deviate from the periodic functions, the smaller r is. Slope of the t_i-i curve represents the average half period of oscillation of the initial portion of P waves, (1/2)T, which can also be calculated using the least square method.

The spatial linearity can be calculated using following method. Considering the seismic data x_{ij} recorded by a certain observatory as three-dimension random variables, where i = 1, 2, 3 and j is sequence number of the sampling points which starts from 1 to the total number of sampling points, N. The expectations and covariance of xij are

$$E_i = \frac{1}{N}\sum_{j=1}^{N} x_{ij} \tag{4}$$

$$C_{ik} = \frac{1}{N}\sum_{j=1}^{N} \left(x_{ij} - E_i\right)\left(x_{kj} - E_k\right) \tag{5}$$

The covariance matrix V can be constructed based on C_{ik} as $V = \{C_{ik}\}$, i, k = 1, 2, 3. From its characteristic equation $(V - \lambda I)n = 0$, its three eigenvalues (from high to low) λ_1, λ_2, λ_3 and their corresponding normal eigenvectors n_1, n_2, n_3 can be determined. n_1 and n_3 are incident directions of P and S waves, respectively and the spatial linearity of the P wave can be defined as:

$$\alpha_1 = 1 - \lambda_2/\lambda_1 \text{ or } \alpha_2 = 1 - \lambda_3/\lambda_1 \tag{6}$$

α_1 and α_2 represent the deviation between actual seismic ray path and its initial ray path. The more highly the paths deviate from each other, the smaller α_1 and α_2 are. Thus, α_1 and α_2 reflect homogeneity of the propagation medium, the higher α_1 and α_2 are, the more homogeneous this medium is, and $\alpha_1 = \alpha_2 = 1$ for the homogeneous medium.

Based on analyzing of several medium and strong earthquakes, it was found that the temporal linearity r, spatial linearity α_1 and α_2, and the half period (1/2)T of the P wave abnormally dropped about one year or longer before the main shock. It was also observed that these anomalies were either intensified or recovered about half years before the main shock. The time span between the "turnover" of the anomalies and the main shock is dependent on the magnitude, epicentral distance, and azimuth angle of the epicenter.

Fig. 3 shows the variations of r, α_1, α_2, and (1/2)T of P waves of the earthquakes occurred from July of 1988 to October of 1989 in Datong, Shanxi. The displayed curves were plotted based on digital data recorded by Baijiatuan station in Beijing, whose epicentral distance is about 200km. In Fig. 3, time window $\Delta\tau = 4$ seconds, sampling interval is 0.025 seconds and total sampling points N is 2000. The entire duration of the abnormal linearity (ΔT) and the time span between the "turnover" of the anomalies and the main shock (ΔT_1) of several earthquakes are listed in Table 4.

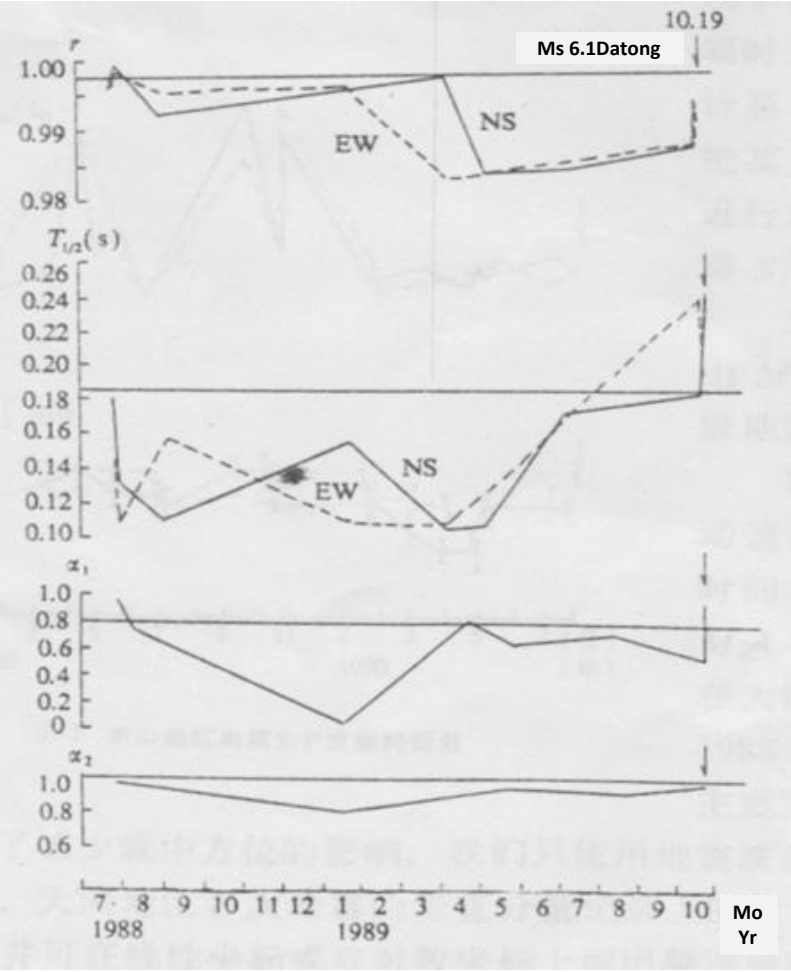

Figure 3.r, α_1, α_2, and (1/2)T of seismic P waves in Datong, Shanxi

Table 4. Duration of the abnormal linearity of waveforms of several earthquakes (ΔT and ΔT_1)

Earthquake	Ms	Recorded by	Epicentral distance	ΔT (months)	ΔT_1 (months)
1989.10.0 in Datong	6.1	Baijiatuan	180-200	14	6
1990.7.23 in Tangshan	4.5	Baijiatuan	150	6	3
1990.2.10 in Changshu	5.1	Sheshan	~80	6	1.5-2
1990.4.26 in Gonghe	6.9	Zhang	~250	>16	6
1975.2.3 in Haicheng	7.3	Yingkou	~10	>20	8
		Dandong	~170	>20	2

VII. Conclusions

This paper describes the correlation between precursory abnormal features of small earthquakes' seismic wave and the impending main shocks. From the examples demonstrated in this paper as well as the author's experience, it is concluded that: (1) the direction of the initial motion of P waves becomes consistent before the main shock and stays in disorder during other time; (2) similarly, the amplitude ratio of small earthquakes would be fairly consistent before the strong main shock; (3) small earthquakes whose seismic waves have rich high-frequency components usually foretell impending strong earthquakes; (4) the temporal linearity, spatial linearity, and the half period of the initial motion of P wave might abnormally drop about one year or longer before the main shock.

The criteria and methods presented in this paper are useful in correctly predicting the future earthquakes and identifying the maximum earthquake from an earthquake swarm. It should also be indicated that significant error may be made by singly using one criterion or feature to predict seismic tendency. Accurate earthquake prediction should be made based on synthetically judging and analyzing the variation of different seismic wave features.

Reference

[1] K.-T. Wu, M.-S.Yue, H.-Y.Wu, X.-L.Cao, H.-T.Chen, W.-Q.Huang, K.-Y.Tian, S.-D. Lu, "Characteristics of Haichen Earthquake Sequence", *ACTA GeophysicaSinica*, 19(2), 1976.

[2] Y. Jin, Y. Zhao, Y. Chen, J.-Q.Yan, Y.-R.Zhuo, "A Characteristic of Hypocentral Dislocation of Foreshocks of Haicheng Earthquake, Liaoning", *ACTA GeophysicaSinica*, 19(3), 1976.

[3] D.-Y. Feng, "Abnormal Amplitude Ratio of S and P Waves of Nearby Earthquake Activities and Their Prediction", *ACTA GeophysicaSinica*, 17(3), 1974.

[4] "Seismic Activity Characteristics of Hellinger Earthquake", Earthquake Team of Inner Mongolia Autonomous Region, *Earthquake*, 5, 1976.

[5] W.-L. Liu and H.-Y. Yu, "Spot Forecast of the M_L4.6 Earthquake Swarm of Shanxi Reservoir, Zhejiang Province occurred on Feb. 9, 2006", *South China Journal of Seismology*, 26(3), 2006, 34-44.

[6] W.-L. Liu and Y.-C.Liu, "Application of Seismic Wave Method in Early Estimation of Wencheng Earthquake", *International Journal of Natural Sciences and Engineering*, 1(2), 2009，121-128.

[7] Y.-Z. Lu, J.-W.Shen, "Study of Seismic Rupture Process", *ACTA GeophysicaSinica*, 23(2), 1980.

[8] T. Johnson, F.T. Wu, C.H. Scholz, "Source Parameters for Stick-Slip and for Earthquakes", *Science*, 179(4070), 1973, 278-280.

[9] A.G. Lindh, C.E. Mantis, "Premonitory Amplitude Changes", Summaries of Technical Reports, VI, 1976, 184-188.

[10] M.A. Sadovsky, I.L. Nersesov, S.K. Nigmatullaev, L.A. Latynina, A.A. Lukk, A.N. Semenov, I.G. Simbireva, V.I. Ulomov, "The Processes Preceding Strong Earthquakes in Some Regions of Middle Asia", *Tectonophysics*, 14(3-4), 1972, 295-307.

[11] M.A. Sadovsky, I.L. Nersesov, "Forecasts of Earthquakes on the Basis of Complex Geophysisical Features", *Tectonophysics*, 23(3), 1974, 247-255.

[12] M. Ishida, H. Kanamori, "Temporal Variation of Seismicity and Spectrum of Small Earthquakes Preceding the 1952 Kern County, California, Earthquake", *Bulletin of the Seismological Society of America*, 70(2), 1980, 509-527.

[13] C.-Z. Zhu, R.-B.Shi, S.-L.Luo, Z.-W.An, "Preliminary Study of Spectra of Microshocks in the Region of Xikeer, Xinjiang", *ACTA GeophysicaSinica*, 18(4), 1975.

[14] C.-Z. Zhu, C.-H.Fu, S.-L.Luo, "Focal Parameters of Micro Earthquakes Occurred before and after Tangshan M_L7.8 Earthquake", *ACTA GeophysicaSinica*, 20(4), 1977.

[15] .-Y. Feng, G.-Y.Wu, H.-R.Chen, R.-Z.Guo, X.-J.Yu, W.-G. Ding, "Application of Indicator of Dynamic Characteristics of Seismic Waves in Short-Term Earthquake Prediction", *Earthquake*,1(1), 1994.